

## Supplementary Information

### Molecular dynamics simulation of thermotropic bolaamphiphiles with a swallow-tail lateral chain: Formation of cubic network phases

Y. Sun, P. Padmanabhan, M. Misra, and F.A. Escobedo

School of Chemical and Biomolecular Engineering, Cornell University, Ithaca, NY 14853

#### S1 Network-skeleton analysis

As mentioned in the main text, we implement a network-skeleton analysis to help us characterize the topology of any network that the rigid rods in the TBAs may be forming. In such a skeleton, points represent nodes and lines represent struts. In the coarse-grained model, each rigid rod consists of two type 1 beads and four type 2 beads. In the network, each node is a cluster of type 1 beads, and each strut is a cluster of type 2 beads (which also form the inner sections of the rigid rods). Here, we provide the main steps to perform this analysis:

1. Classify all the type 1 beads into different nodes. For each such bead  $i$ , we define its neighboring beads as the beads within the cutoff distance,  $d_{\text{cutoff}}$ , chosen to be  $1.3\sigma$ . Based on the condition that any bead from a cluster can find all its neighboring beads in the same cluster, we classify the beads into different clusters, so that each bead only belongs to one cluster. A pseudocode is shown in Figure S1.1.

2. Check and correct the nodal clusters from step 1. During classification, some beads may be misclassified, and a correction be needed. This correction is based on the number of beads in each cluster (called the cluster size). We set an acceptable range (based on our experience with many cases) for the cluster size with a minimum of 9 and the maximum of 40. If a cluster whose size is smaller than the minimum, all beads in this cluster will be reassigned to their nearest cluster whose size is in the acceptable range. If a cluster size is larger than the maximum, we divide it into several clusters based on the number of neighboring beads of a given bead (called the local coordination number  $N_{co}$ ). We reclassify the beads in this cluster, whose  $N_{co} > 3$ , into several clusters using the method in step 1. We reassign the beads in this cluster, whose  $N_{co} < 3$ , to their nearest cluster whose size is in the acceptable range. The algorithm is illustrated in Figure S1.2 as pseudocode. After the correction, each cluster represents a node in the network. Hence, the number of such clusters represents the number of nodes in the network ( $N_{\text{node}}$ ).

3. Classify all the rigid rods into different struts. After step 2, the two type 1 beads from the same rigid rod must have been classified into two different nodes. Thus, for each rigid rod, we know which two nodes it connects. All the rigid rods, which merge into the same two nodes at their ends, are classified as one strut. After all rods have been sorted out, we collect the information on the number of rigid rods in each strut ( $N_{\text{rod-strut}}$ ).

4. Determine the neighboring nodes for each node classified in step 2. After step 3, we know which two nodes are

connected by the same strut. Hence, any two nodes connected by the same strut are treated as neighboring nodes. The number of the neighboring nodes of a given node in the network is the valence ( $v$ ) of that node.

5. Draw the skeleton of the network. Each node is represented by the center of mass of the type 1 beads belonging to the same node (as per the classification in step 2). Each strut is represented by a straight line connecting the two corresponding neighboring nodes (as per the information collected from step 4).

```
Algorithm start
Declare a node ID to be assigned for each type 1 bead
called NodeID
Declare an array to store the node ID for each type 1 bead
called Bead-IDs
Initiate all members in Bead-IDs to be 0
Count the number of 0 in array Bead-IDs called N0
NodeID = 1

Do
  Set a member in Bead-IDs which is 0 to be NodeID
  Count the number of NodeID in array Bead-IDs called
  N_pre

  Do
    For member i in Bead-IDs which is 0
      For member j in Bead-IDs which is NodeID
        Calculate the distance between bead i and bead j
        called dij
        If dij < dcutoff
          Bead-IDs[i] = NodeID
        Endif
      Endfor
    Endfor
  Endfor
  Count the number of NodeID in array Bead-IDs again
  called N_apt
  Until N_pre == N_apt
  Enddo

NodeID += 1
Count N0 again
Until N0 = 0
Enddo
Algorithm end
```

Figure S1.1 Pseudocode for the classification in step 1 of the network-skeleton analysis.

## S2 Additional data & analysis for $\eta = 0.45$

As indicated in the main text, most of our simulations were performed at a packing fraction of  $\eta = 0.45$ . The network skeleton analysis and the mobility coefficient are used to further characterize the structure and dynamics of different 3D-periodic phases that were observed. In this section, we provide additional data collected from the network skeleton and the mobility coefficient.

```

Algorithm start
Get size of every cluster from step 1
Set the minimum of the cluster size as size_low
Set the maximum of the cluster size as size_high

If a cluster whose size is in [size_low, size_high]
  Tag this cluster as normal_cluster
Else if a cluster whose size is smaller than size_low
  Tag this cluster as small_cluster
Else if a cluster whose size is bigger than size_high
  Tag this cluster as large_cluster
Endif

For the cluster tagged as the small_cluster
  For the beads in this cluster called bead k
    Calculate the distance between bead k and all beads
    belongs to any normal_clusters
    Find the minimum distance and the related normal_cluster
    (called l)
    Reassign bead k to this normal_cluster l
  Endfor
Endfor

For the cluster tagged as the large_group
  For the beads in this group
    Calculate the coordination number  $N_{co}$  of this bead based
    on the cutoff distance,  $d_{cutoff}$ 
    If  $N_{co}$  is smaller than 3
      Tag this bead as bridge_bead
    Else:
      Tag this bead as cluster_bead
    Endif
  Endfor

  Reclassify all the beads tagged as cluster_bead into several
  culsters using method in Figure S1
  For the beads tagged as bridge_bead called bead x
    Calculate the distance between bead x and all beads
    belongs to any normal_cluster
    Find the minimum distance and related normal_cluster
    (called y)
    Reassign bead x to this normal_cluster y
  Endfor

Endfor
Algorithm End

```

Figure S1.2 Pseudocode for the correction in step 2 of the network-skeleton analysis.

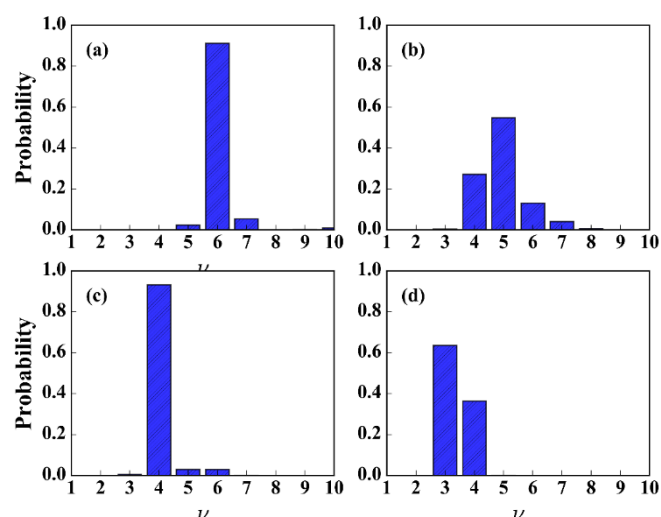


Figure S2.1 Population distribution of the nodal valence ( $v$ ) for TBA molecules with different length of the lateral chain. (a)  $N_{fix} = 5$ ; (b)  $N_{fix} = 7$ ; (c)  $N_{fix} = 9$ ; (d)  $N_{fix} = 17$ .

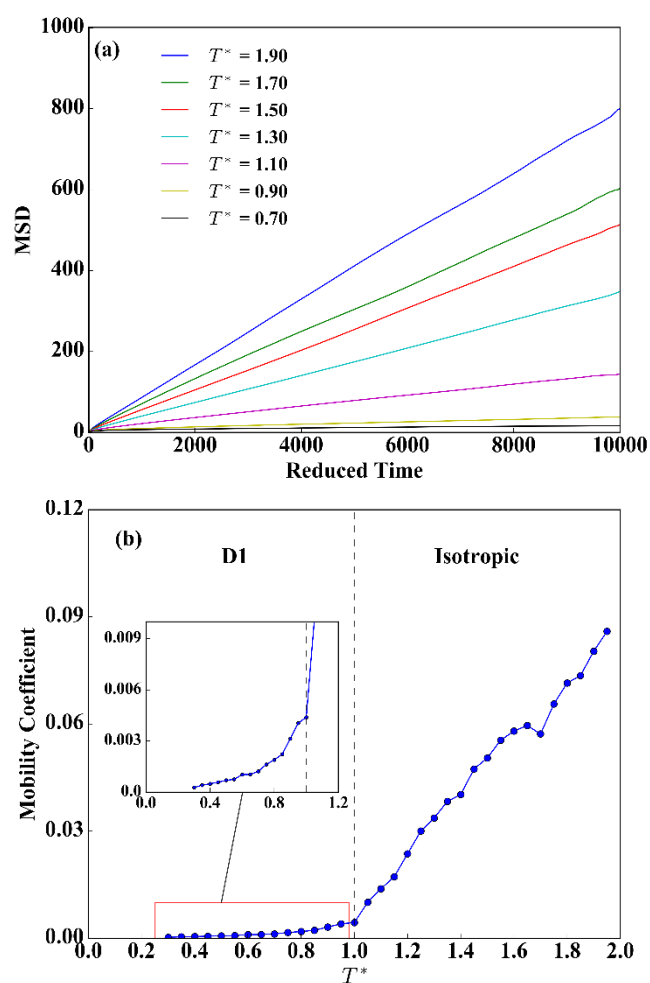


Figure S2.2 (a) Mean-squared displacement as a function of time for different simulation temperature. (b) The mobility coefficient for  $N_{fix} = 11$  TBAs and  $N = 600$  as a function of temperature. “D1” refers to the “single” diamond phase.

Table S2.1 Average properties of the G phase network for the different lengths of the lateral chain.  $N$  is the number of molecules in the simulation box;  $L_{\text{box}}$  is the length of the simulation box;  $L_{\text{ucell}}$  is the length of the calculated unit cell;  $T^*$  is the temperature range where the G phase is detected;  $N_{\text{node}}$  and  $N_{\text{strut}}$  are the number of nodes and struts of the network in the box;  $N_{\text{rod-strut}}$  is the average number of rigid rods in a strut of the network.

$N_{\text{flx}}$	$\phi_{\text{flx}}$	$N$	$L_{\text{box}}$	$L_{\text{ucell}}$	$T^*$	$N_{\text{node}}$	$N_{\text{strut}}$	$N_{\text{rod-strut}}$
19	0.752	300	20.66	20.66	0.30 - 0.95	16	24	12.5
21	0.771	300	21.18	21.18	0.30 - 0.90	16	24	12.5
23	0.786	300	21.69	21.69	0.30 - 0.95	16	24	12.5
25	0.800	300	22.18	22.18	0.30 - 1.00	16	24	12.5
27	0.812	300	22.64	22.64	0.30 - 1.05	16	24	12.5
29	0.823	300	23.08	23.08	0.30 - 1.00	16	24	12.5

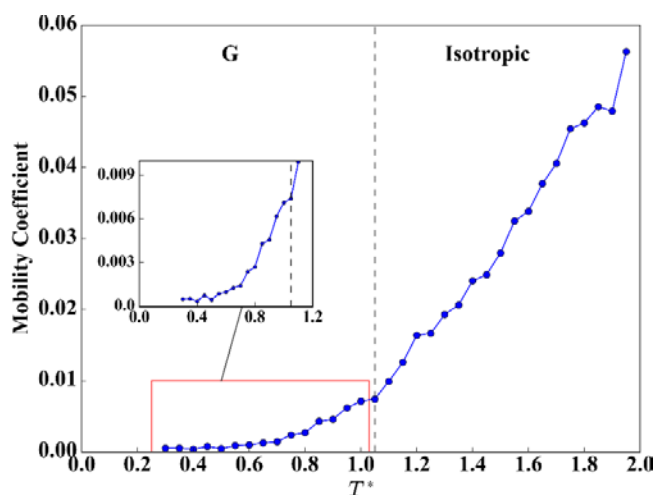


Figure S2.3 The mobility coefficient for  $N_{\text{fix}} = 19$  TBAs with  $N = 300$  as a function of temperature. “G” refers to the double gyroid phase.

### S3 Simulation results for TBAs at the packing fraction of $\eta = 0.5$

A global phase diagram in terms of reduced temperature and the volume fraction of the lateral chain ( $\phi_{\text{flx}}$ ) is presented in Figure S3.1. Compared with the simulation results at  $\eta = 0.45$  shown in Figure 3, at  $\eta = 0.5$  we obtained essentially the same morphologies including the square honeycomb column, the “single” diamond (D1), the double gyroid (G) and the hexagonal axial-bundle column. The main difference is that for  $\eta = 0.5$  the temperature range of mesophase stability is wider. By increasing the packing fraction, the pressure of the system and the tendency of the molecules to order (*e.g.*, for the rigid rods to align) are both increased, which shifted the transition point between isotropic phase and LC phase to higher temperatures. The square honeycomb columnar and the D1 phase are observed at the same  $\phi_{\text{flx}}$  for  $\eta = 0.5$  and  $\eta = 0.45$ . Our simulations did not detect the “single” plumber’s nightmare (P1) phase at  $\eta = 0.5$ , which was observed at  $\eta = 0.45$ . The G phase was detected for  $0.752 \leq \phi_{\text{flx}} \leq 0.786$  at  $\eta = 0.5$ , which is a narrower range than that observed for  $\eta = 0.45$ . The axial-bundle columnar phase was detected for lower  $\phi_{\text{flx}}$  values at  $\eta = 0.5$ .

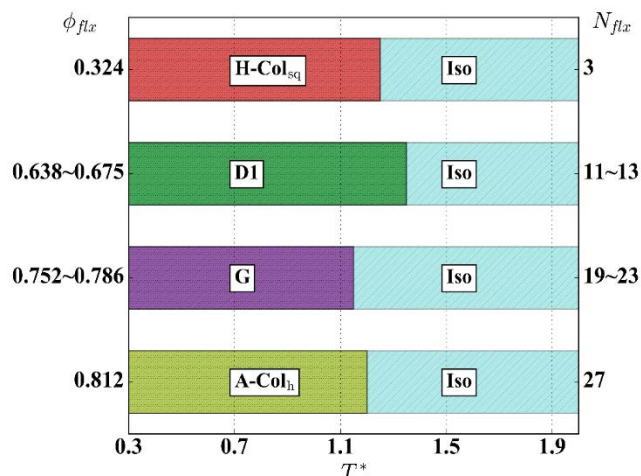


Figure S3.1 Morphologies obtained in simulations for the bolaamphiphile molecule with a swallow-tail lateral chain at packing fraction of  $\eta = 0.5$  with respect to temperature and the volume fraction of the lateral chain. Morphology description: “Iso” refers to isotropic, “H-Col<sub>sq</sub>” to square honeycomb column, “D1” to “single” diamond network, “G” double gyroid, “A-Col<sub>h</sub>” axial-bundle column with hexagonal symmetry and plan group  $p6mm$ .

### S4 Morphologies of rigid rod bundles

The morphology of the rigid rod bundles was studied after classifying all the rigid rods into different struts through the skeleton-network analysis for the P1, D1 and G phases. Figure S4.1 confirms that each strut contains only one bundle of rods in the P1 and D1 phases, while each strut contains two successive coaxial bundles of rods in the G phase. To get a general idea of how these rigid rods pack in the bundles, we focused on the cross section of each bundle. Such a cross section was found to exhibit different morphologies depending on the size of the bundle ( $N_{\text{bund}}$ ). For the bundles with  $N_{\text{bund}} = 3, 4, 5$ , only one close-packed cross section was observed for each case (see Figure S4.2). For the bundles with  $N_{\text{bund}} = 6$ , three morphologies of the cross section were observed: rectangular, triangular, and hexagonal as shown in Figures S4.3(a), (b) and (c), respectively. In the latter (Figure S4.3(c)) one rigid rod is surrounded by five other rods and the long axis of each rod is not parallel to each other to allow the lateral chain attached to the center rod to access to the internetwork continuous phase.

In the Figure S4.3(c), the center rod and its lateral chain are colored pink and yellow, respectively. Figures S4.4 and S4.5. show some of the morphologies observed in our simulations for

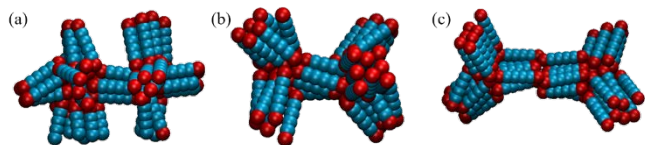


Figure S4.1 Sample snapshots of the different morphologies of a connecting strut between neighboring nodes. (a) P1 network; (b) D1 network; (c) G network.

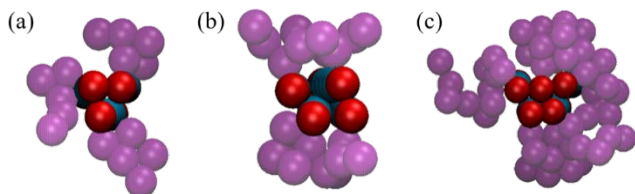


Figure S4.2 Sample snapshots of the different cross sections of rigid rod bundles with  $N_{\text{bund}} = 3, 4, 5$ . The type 1 beads are colored red, the type 2 beads are colored blue, and type 3 beads are colored purple.

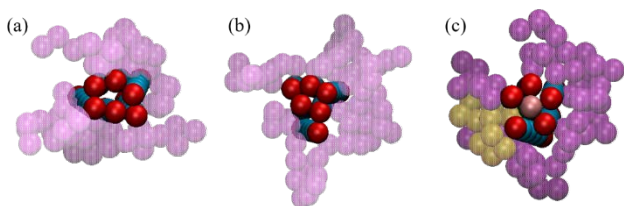


Figure S4.3 Sample snapshots of the different cross sections of rigid rod bundles with  $N_{\text{bund}} = 6$ . The type 1 beads are colored red and pink, the type 2 beads are colored blue and green, and the type 3 beads are colored purple and yellow.

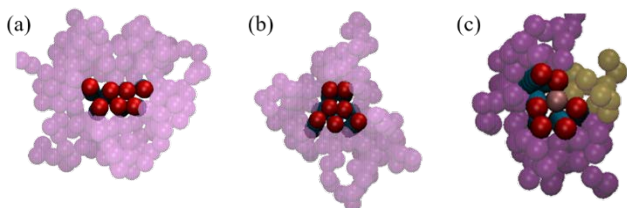


Figure S4.4 Sample snapshots of the different cross sections of rigid rod bundles with  $N_{\text{bund}} = 7$ .

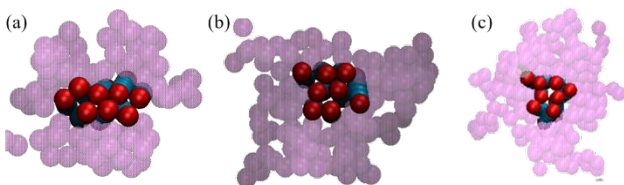


Figure S4.5 Sample snapshots of the different cross sections of rigid rod bundles with  $N_{\text{bund}} = 8$ .

the bundles with  $N_{\text{bund}} = 7, 8$ .

## S5 Simulations of TBAs of different molecular architecture

To understand the relationship between the architecture of TBA side-chain and the mesophase they form, a series of simulations were performed at  $\eta = 0.45$  for two types of molecules: TBAs with a swallow-tail lateral chain (as described in full in the main text) and TBAs with a linear lateral chain. As shown in Figure S5.1, for the case of  $N_{\text{fix}} = 5, 11$  and  $19$ , TBAs with either linear or swallow-tail lateral chains tend to assemble into different morphologies. For the case of  $N_{\text{fix}} = 5$ , we find that TBAs with a linear lateral chain forms the hexagonal honeycomb columnar (H-Col<sub>h</sub>) phase for  $T^* \leq 1.05$ , while the TBA with a swallow-tail lateral chain forms the P1 phase for  $T^* \leq 0.80$ . For the case of  $N_{\text{fix}} = 11$ , we find that TBAs with a linear lateral chain forms the lamella (L) phase for  $T^* \leq 1.0$ , while the TBA with a swallow-tail lateral chain forms the D1 phase for  $T^* \leq 0.95$ . For the case of  $N_{\text{fix}} = 23$ , we find that TBAs with a linear lateral chain forms the lamella (L) phase for  $T^* \leq 1.35$ , while the TBA with a swallow-tail lateral chain forms the G phase for  $T^* \leq 0.9$ .

To investigate the energetic and entropic effects for the same lateral chain architecture in different morphologies, the following method was implemented as illustrated for the  $N_{\text{fix}} = 23$  case below. Figure S5.1 shows the L and the G phase that were spontaneously formed for the linear lateral chain TBA (L-TBA) and the swallow-tail lateral chain TBA (S-TBA), respectively. To allow the S-TBA to form the L phase, we take the configuration of the L phase collected from L-TBA, and temporarily “freeze” the position of the rigid rods (*i.e.* by zeroing out the force and torque on the rigid rods). Then we change the harmonic bond between the rigid rod and the lateral chain so as to change the chain topology in a stepwise manner. At first, this bond connects the rigid rod and the first bead in the lateral chain (the architecture of the L-TBA, shown in the first picture in Figure S5.2(a)). We then turn off this bond and add a bond between the rod and the second bead in the lateral chain (see Figure S5.2(b)). We then let the system to equilibrate with this new lateral chain architecture over a period of  $t^* = 5000$ .

Molecular Architecture	$N_{\text{fix}} = 3$	$N_{\text{fix}} = 5$	$N_{\text{fix}} = 11$	$N_{\text{fix}} = 23$
TBA with a linear lateral chain				
TBA with a swallow-tail lateral chain				

Figure S5.1 Morphologies obtained for different molecular architecture and various the lengths of the lateral chain. For clarity, only the rigid rods are shown, and only the skeleton of the network is shown in the P1 and D1 phase. Except for the G phase, the type 1 beads are colored red, the type 2 beads are colored blue. For the G phase, its two distinct non-intersecting networks are colored red and blue, respectively.

We repeat this process to gradually move the connection from one end to the center of the lateral chain (see Figure S5.2(c) (d)). Once the rigid rod is connected to the center bead of the lateral chain, we obtain the architecture of the S-TBA in the L phase. Similarly, to allow the L-TBA to form the G phase, we simply “freeze” the rigid rods in the G phase, and change the connecting bead of the lateral chain from the center bead to one of the end beads (see Figure S5.2 panels (e), (f), (g) and (h)). To compare the results at the same temperature, we also “freeze” the rigid rods in different morphologies, and gradually change the temperature of the lateral chains toward the target temperature. In this method, the rigid rods are kept “frozen” throughout the whole procedure, to avoid destroying the desired morphology for a specific molecular architecture at a target

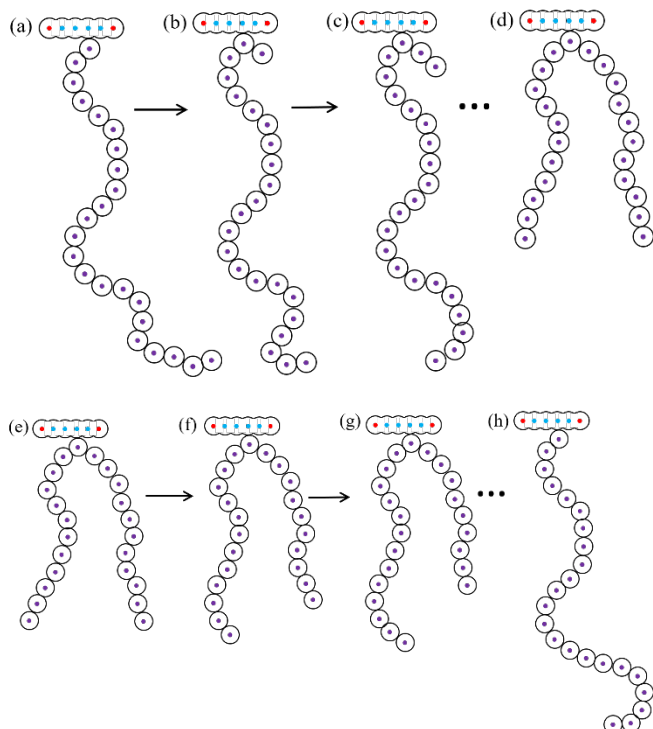


Figure S5.2 Scheme for changing the lateral chain architecture while “freezing” the rigid rod. (a) to (c) Architecture mutates from L-TBA to S-TBA; (d) to (f) architecture mutates from S-TBA to L-TBA.

temperature.

To characterize the conformational behavior of the lateral chain, the end-to-end distance is calculated as illustrated in Figure S5.3. For the linear lateral chain, the end-to-end distance is defined as the distance between the first and last of the flexible beads. For the swallow-tail lateral chain, the end-to-end distance for each branch is considered, which is defined as the distance between the bead connecting the two branches and the last bead in each branch. Statistics are collected at time intervals of  $\Delta\tau = 200$  over a period of  $t^* = 100000$ , while the rods are frozen to preserve the desired morphology.

In this section, we also provide additional data collected from the system of  $N_{\text{fix}} = 5, 11$ . For the case of  $N = 400$  and  $N_{\text{fix}} = 5$ ,

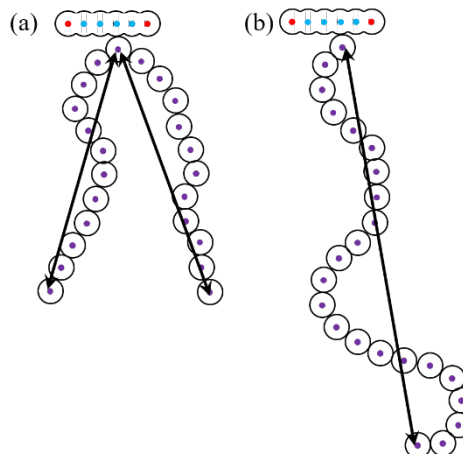


Figure S5.3 Definition of the end-to-end distance of the lateral chain for the different architectures: (a) TBA with linear lateral chain; (b) TBA with swallow-tail lateral chain.

the energetic and entropic preference were investigated at  $T^* = 1.10$  for the same lateral chain architecture but in the H-Col<sub>h</sub> and P1 phase. As shown in the Table S5.2, the  $U_{\text{total}}$  in the H phase is always more negative than that in the P1 phase, indicating an energetic preference for the H-Col<sub>h</sub> phase over the P1 phase regardless of the molecular architecture, and that P1 phase must have a larger interface. Figure S5.4 confirms that the lateral chain of the S-TBA need to be significantly stretched to form the H-Col<sub>h</sub> phase, while the L-TBA doesn't show a marked entropic preference for the H-Col<sub>h</sub> phase over the P1 phase. In summary, for the S-TBA, the P1 phase is more favorable than the H phase for entropic reasons (the relief of a chain stretching) despite a larger interfacial energy. In contrast, for L-TBA the H-Col<sub>h</sub> phase is more favorable than the P1 phase because of its lower interfacial energy, there being no marked entropic preference for either phase.

For the case of  $N = 600$  and  $N_{\text{fix}} = 11$ , the energetic and entropic preference were investigated at  $T^* = 1.20$  for the same lateral chain architecture but in the L and D1 phase. The results in Table S5.3 and Figure S5.5, show that for the S-TBA the D1 phase is more favorable than the L phase for entropic reasons (the relief of a chain stretching) despite a larger interfacial energy. In contrast, for L-TBA the L phase is more favorable than the D1 phase because of its lower interfacial energy, there being no marked entropic preference for either phase.

Table S5.2 Total potential energy per bead ( $U_{\text{total}}$ , in units of  $\epsilon$ ) of the TBA with  $N_{\text{fix}} = 5$  for two distinct structures.  $U_{\text{total}}(\text{swallow-tail})$  is for the TBA with a swallow-tail lateral chain;  $U_{\text{total}}(\text{linear})$  is for the TBA with a linear lateral chain.

	P1	H-Col <sub>h</sub>
$U_{\text{total}}(\text{swallow-tail})$	-0.429	-0.489
$U_{\text{total}}(\text{linear})$	-0.443	-0.546

Table S5.3 Total potential energy per bead ( $U_{\text{total}}$ , in units of  $\varepsilon$ ) of the TBA with  $N_{\text{fix}} = 11$  for two distinct structures.  $U_{\text{total}}(\text{swallow-tail})$  is for the TBA with a swallow-tail lateral chain;  $U_{\text{total}}(\text{linear})$  is for the TBA with a linear lateral chain;

	D1	L
$U_{\text{total}}(\text{swallow-tail})$	-0.463	-0.499
$U_{\text{total}}(\text{linear})$	-0.472	-0.525

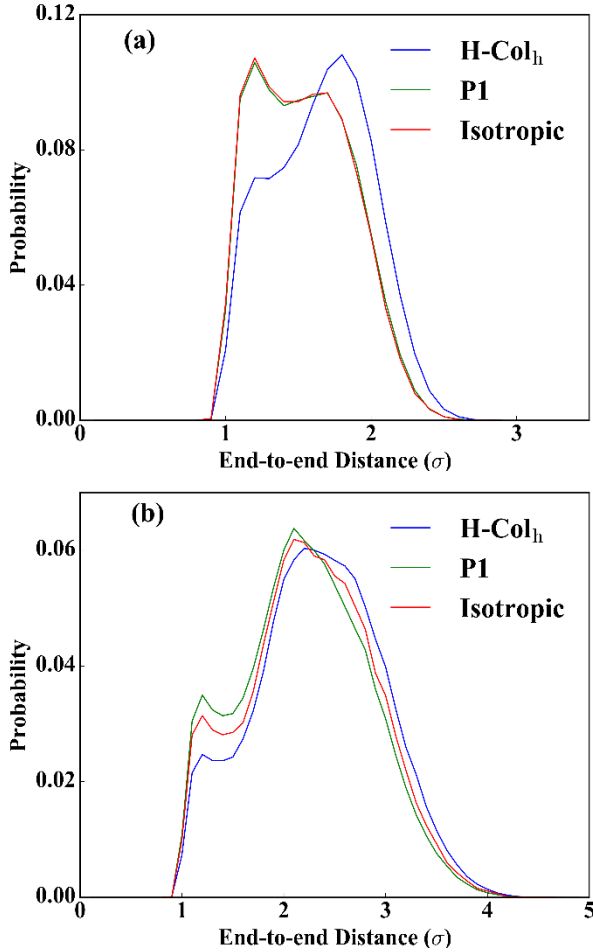


Figure S5.4 End-to-end distance for TBAs with  $N_{\text{fix}} = 5$ . (a) The TBA with a swallow-tail lateral chain in three distinct structures (isotropic,  $H\text{-Col}_h$  and P1); (b) The TBA with a linear lateral chain in the same three distinct structures.

### S6 (movie; see file P1.avi) Liquid crystalline character of the P1 phase

This movie tracks a group of rigid rods over time in the P1 phase of a  $N_{\text{fix}} = 5$  system at equilibrium at  $T^* = 0.60$ . At the beginning, the highlighted rigid rods belong to the same strut but later on one of these rods hops to another strut, while the rest rods still vibrate around the original strut.

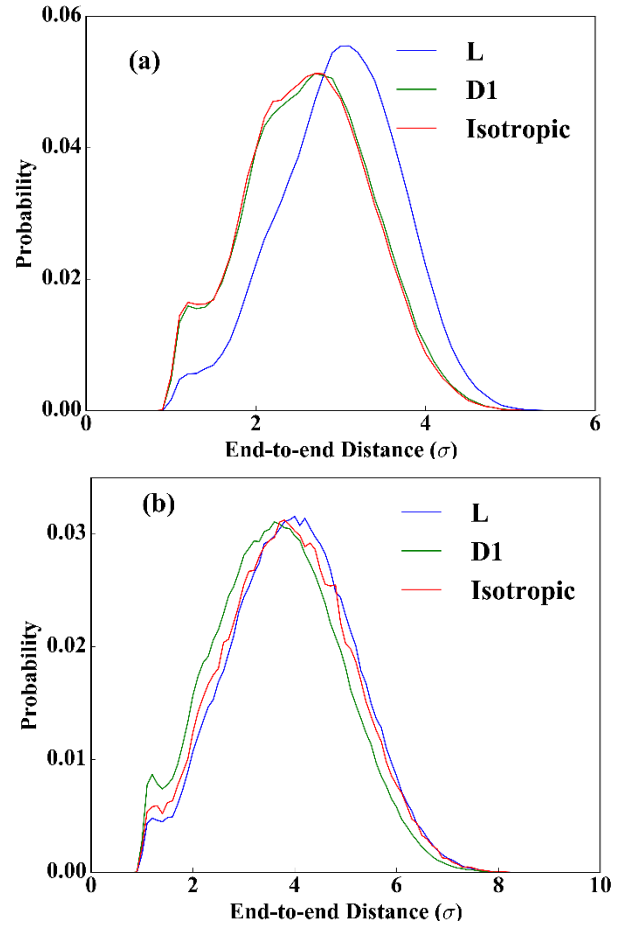


Figure S5.5 End-to-end distance for TBAs with  $N_{\text{fix}} = 11$ . (a) The TBA with a swallow-tail lateral chain in three distinct structures (isotropic, L and D1); (b) The TBA with a linear lateral chain in three distinct structures.

### S7 (movie; see file D1.avi) Liquid crystalline character of the D1 phase

This movie tracks a system with  $N_{\text{fix}} = 11$  at equilibrium at  $T^* = 0.80$  (LC phase). It highlights one clusters of rigid rods which at the beginning belong to the same strut. During the movie, one of these highlighted rigid rods hops to another strut, while the rest rods still vibrate around the original strut.